Analytical Methods

Accepted Manuscript

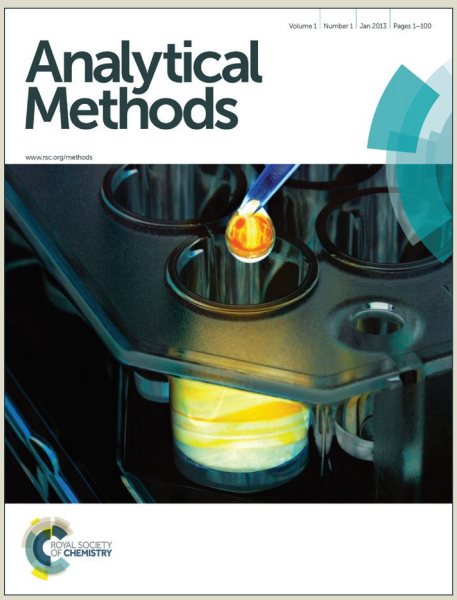

This is an *Accepted Manuscript*, which has been through the Royal Society of Chemistry peer review process and has been accepted for publication.

Accepted Manuscripts are published online shortly after acceptance, before technical editing, formatting and proof reading. Using this free service, authors can make their results available to the community, in citable form, before we publish the edited article. We will replace this *Accepted Manuscript* with the edited and formatted *Advance Article* as soon as it is available.

You can find more information about *Accepted Manuscripts* in the Information for Authors.

Please note that technical editing may introduce minor changes to the text and/or graphics, which may alter content. The journal's standard Terms & Conditions and the Ethical guidelines still apply. In no event shall the Royal Society of Chemistry be held responsible for any errors or omissions in this *Accepted Manuscript* or any consequences arising from the use of any information it contains.

ROYAL SOCIETY OF CHEMISTRY

www.rsc.org/methods

Characterization of TLR4/MD-2-modified Au sensor surfaces; Towards the detection of molecular signatures of bacteria

Kaveh Amini[1], Iraklii I. Ebralidze[1], Nora W.C. Chan[2], Heinz-Bernhard Kraatz[1] *

[1]*Department of Physical and Environmental Sciences, University of Toronto Scarborough, Toronto, ON, Canada*

[2]*Defence Research and Development Canada - Suffield Research Centre PO Box 4000 Station Main, Medicine Hat, Alberta, T1A 8K6, Canada*

* Corresponding author email: bernie.kraatz@utoronto.ca; fax: (+1) 416-287-7279

Abstract

Lipopolysaccharid (LPS), also known as endotoxin can be fatal even at low concentrations. As a result, the development of novel methodologies for LPS detection has been continuously in the focus of research. The biosensors, which employ a bio-recognition element on a transducer surface are in the cutting edge of these novel technologies. In this report, Au surfaces modified with TLR4/MD-2 through Lip-NHS linkers with an ultimate potential application as biosensors for LPS detection have been characterized and investigated using X-ray photoelectron spectroscopy, Quartz crystal microbalance and electrochemical techniques. Also the interaction between TLR4/MD-2 immobilized on Au surfaces with LPS has been studied to evaluate the possibility of LPS detection.

Introduction

Pathogen detection still relies on the traditional microbiological and biochemical methods including lengthy culturing procedures. These methods are pretty time-consuming and also they generally focus on determination of only *E. coli* as an indicator bacterium of fecal contamination. Other newly introduced methods employed for pathogen detection are mainly based on immunofluorescent assay, Polymerase Chain Reaction (PCR) or DNA sequencing techniques. These techniques in addition to being time-consuming are also complex and expensive. Moreover, these techniques require high expertise and are limited to only laboratory use and not on-site applications.[1-2] In recent years, development of label-free biosensing techniques has attracted a significant attention. These methods include optical sensors[3], Photoelectrochemical immunosensors[4], Fluorescence-based sensors[5], sensors based on quartz crystal microbalance[6], sensors utilizing the surface plasmon resonance technology[7], Electrochemical Impedance Spectroscopy (EIS)-based sensors[8], etc. These label-free detection methods have many advantages such as being easy to use, easy to miniaturize, fast and sensitive enough for detection of biological molecules such as DNA[9], bacteria[10], viruses[11], proteins[12] and lipopolysaccharide (LPS).[13] LPS, also known as endotoxin, being the major component of Gram-negative bacterial cell wall is shredded from bacteria during their lysis and is responsible for their toxicity. Detection of LPS is of great importance not only because its presence can be an indication of

Gram-negative bacterial contamination which could lead to sepsis, but also because of its high toxicity. The standard method currently employed for LPS detection is Limulus Amebocyte Lysate (LAL) test.[2] Although this method is very sensitive and can be used in quantitative analysis, its low reproducibility, its dependence on pH and the interference from chelators and proteases are its significant disadvantages.[14] Recently some new techniques based on biosensor concept for LPS detection with better sensitivity and selectivity have been introduced. These techniques include utilizing luminescence depolarization along with sol-gel process[15], cyclic voltammetry[16], differential pulse voltammetry[17] and Impedance-based sensors[18]. Sensors based on EIS use a bio-recognition element specific towards the target analyte immobilized on a transducer surface.

Innate immune system of higher organisms provides efficient defense against infections caused by pathogens. The tools employed by the innate immunity to perform this task are a family of type I transmembrane glycoproteins called Toll-Like Receptors (TLRs).[19] TLRs recognize molecular patterns or signatures of pathogens which are broad but highly conserved and are also absent among the host organism's molecules. TLR4 was identified as the receptor for LPS in 1998.[20] It has an extracellular domain (608 residues), a single transmembrane domain and an intracellular domain (187 residues).[21-22] MD-2, which only has an extracellular domain without the transmembrane and intracellular domains associates with the extracellular domain of TLR4 and forms the TLR4/MD-2 complex that interacts with LPS.[23] LPS is an outer membrane

glycolipid of Gram-negative bacteria which serves as the molecular signature of them and initiates the innate immune response by interacting with TLR4/MD-2.[24] LPS is composed of three parts: (i) a hydrophobic lipid A component (ii) a hydrophilic core polysaccharide and (iii) an O-antigen side chain. The lipid A portion of LPS is the conserved part of it, makes LPS the molecular pattern for Gram-negative bacteria and is responsible for triggering immune response to LPS.

The interaction and binding of LPS to the TLR4/MD-2 receptor, makes this protein complex a potential bio-recognition element for detection of LPS in different sensor technologies.

In the present study, Au surfaces modified with TLR4/MD-2 are characterized and the interaction between the immobilized TLR4/MD-2 and LPS has been investigated using EIS. An understanding of this interaction provides significant information about the possibility of employing TLR4/MD-2 as a bio-recognition element for LPS detection. TLR4/MD-2-modified EIS-based sensors can provide a fast, easy to use and low-cost platform for detection of LPS (endotoxin) as a toxic matter by itself or as an indicator of Gram-negative bacterial contamination in environment, clinical and food samples.

Experimental section

Reagents

The TLR4/MD-2 complex and Lipopolysaccharide (LPS) samples from *E. coli* and *Salmonella* were obtained from R&D systems (Minneapolis, MN). HCl, NaOH, H_2SO_4, $K_4[Fe(CN)_6]$ and

$K_3[Fe(CN)_6]$ were purchased from Sigma Aldrich (St. Louis, MO). Ultrapure water (18.3 MΩ cm) using a Milli-Q system (Millipore, MA) was used to prepare all buffers. Boric acid was from BioShop (Burlington, ON). Lipoic acid N-hydroxysuccinimide ester (Lip-NHS) linker was synthesized as described before.[25]

Electrochemistry

Microcrystalline gold disk electrodes (0.2 cm diameter) from CH Instruments (Austin, Texas) and a CHI 660C potentiostat (CH Instruments, Austin, Texas) were employed for electrochemical experiments. A three electrode setup consisting of an Ag/AgCl 3 M KCl as the reference, Pt wire as the auxiliary and TLR4/MD-2-modified gold electrode as the working electrode was used. A salt bridge was used to connect the reference electrode. All measurements were performed in $K_4[Fe(CN)_6]$ and $K_3[Fe(CN)_6]$ (5mM each) in 100 mM borate buffer (pH 7.4) solution. ZSimpWin 2.0 (EChem Software) was employed to analyze and fit the EIS experimental data to the appropriate equivalent circuit.

Electrode cleaning

Gold electrodes were incubated in piranha solution (H_2SO_4–H_2O_2 3:1 (v/v)) for 20 s and rinsed with H_2O followed by being polished with alumina slurry (0.1 mm and 0.05 mm, respectively) for 2 min. After rinsing the electrodes with H_2O, they were electrochemically cleaned by cycling in the range of -2 to 0 V vs. Ag/AgCl in 0.5 M KOH and then cycling in the range of 0 to +1.5 V in 0.5 M H_2SO_4.

Modification of electrodes with TLR4/MD-2 complex

The immobilization of TLR4/MD-2 complex on Au surfaces was achieved through a previously introduced method.[26]

The steps of modification of Au surfaces by TLR4/MD-2 through Lip-NHS linkers have been schematically depicted in Scheme 1. The successful completion of each modification step was confirmed using Electrochemical Impedance Spectroscopy and Square Wave Voltammetry (Fig. 1). Cleaned electrodes were incubated in 2 mM ethanolic solution of Lip-NHS for 48 h at 4 °C. The electrodes were then rinsed with ethanol and dried under N_2 flow and incubated in 5 mg mL^{-1} TLR4/MD-2 protein solution in 100 mM Borate buffer pH 7.4 for 48 h at 4 °C. After rinsing with H_2O, 1M ethanolamine in 50 mM Tris buffer pH 8.5 was used to block the electrodes (2 h), and then the electrodes were rinsed with H_2O.

Detection of LPS with TLR4/MD-2 modified Au sensors

The whole detection process has been schematically illustrated in Scheme 1. The TLR4/MD-2 modified electrodes were incubated in LPS solutions from *E. coli* and *Salmonalla* individually at different concentrations of 0.0005, 0.005, 0.05 0.5 and 5 EU mL^{-1} in 100 mM Borate buffer pH 7.4 for 30 min at room temperature (23 °C) while shaking at 400 rpm using a VWR incubating

shaker. Before electrochemical measurements (Electrochemical Impedance Spectroscopy (EIS)) the electrodes were rinsed thoroughly with H_2O to remove any physically adsorbed LPS.

Construction of calibration curves

In order to quantify LPS, calibration curves (R_{ct} vs poly (I:C) concentration) were constructed. The characteristics of the calibration curves for determination of both LPS samples (from *E. coli* and *Salmonalla*) are summarized in Table 1. The lower limit of detection (LOD) was calculated using the expression: $LOD=3SD_b/m$, where SD_b is the standard deviation of the blank and m is the slope of the calibration curve.[27-28]

X-ray photoelectron spectroscopy (XPS)

X-ray photoelectron spectroscopy (XPS) measurements were carried out at the Surface Interface Ontario Center (University of Toronto) on a Thermo Scientific K-Alpha spectrophotometer (ThermoFisher, E. Grinstead) equipped with an Al K_α (1486.6 eV) X-ray source. The typical operating pressure was $<5 \times 10^{-9}$ mbar. The binding energies were referenced to the Au $4f_{7/2}$ peak energy at 84.0 eV. XPS was employed to characterize the TLR4/MD-2-modified gold on silicon surfaces and measure the thickness of the monolayers formed.

Briefly, silicon chips coated with sputtered gold (Ti 6 nm, Au 140 nm, 0.2 cm^2 surface area, fabricated at Nanofabrication Facility, University of Western Ontario) were cleaned for 20 s with

piranha solution (H_2SO_4/H_2O_2 3:1 (v/v)) and rinsed with Millipore water and sonicated in ethanol for 10 min. After drying under N_2 flow, the chips were incubated with an ethanolic solution of 2 mM Lip-NHS for 48 h at 4 °C. Then the gold coated silicon chips were rinsed with ethanol and dried and incubated with 5 μg mL^{-1} TLR4/MD-2 solution in 100 mM borate buffer pH 7.4 for 48 h at 4°C and then blocked in 1 M ethanolamine in 50 mM Tris buffer pH 8.5 (2 h). The TLR4/MD-2-modified and blocked chip was incubated in 5 EU mL^{-1} LPS (*E. coli*) and then the surface was thoroughly washed with Millipore water several times to remove any physically adsorbed LPS and dried under N_2 flow.

Quartz Crystal Microbalance (QCM)

Quartz-crystal microbalance (QCM) measurements were performed using a CHI 660C (CH Instruments, Austin, Texas). 7.995 MHz plates oscillating at the fundamental frequency were employed for QCM studies.

Results and Discussion

Electrochemical characteristics of the modified electrodes

SWV (Fig. 1A) and EIS (Fig. 1B) in 100 mM borate buffer solution containing 5.0 mM of $[Fe(CN)_6]^{3-/4-}$ were used for the step by step characterization of the modification process of the gold electrodes by TLR4/MD-2. Each step of modification led to a significant increase in the charge-transfer resistance (R_{ct}) (Fig. 1B). For the bare Au electrode, a straight line as an indicator

of the fast charge-transfer process was observed. Subsequently, the R_{ct} value was dramatically enhanced after immobilization of the insulating Lip-NHS and TLR4/MD-2 layers and blocking of the surface with 1 M ethanolamine in 50 mM tris buffer pH 8.5. Also a decrease in the current due to immobilization of insulating layers of Lip-NHS, TLR4/MD-2 protein complex and surface blocking was observed in the SWVs of $[Fe(CN)_6]^{3-/4-}$ at different stages of the electrode modification (Fig. 1A). The EIS results were well in agreement with those of the SWV, confirming the success of each step of the modification.

Electrochemical analysis of electron transfer

CV is an effective technique for detection and analysis of the electron transfer between a solution and an electrode which employs a redox probe such as $K_3[Fe(CN)_6]^{3+/4+}$. This electron transfer occurs either by tunneling through the insulating layer immobilized on the Au electrode (Lip-NHS, TLR4/MD-2) or through the defects in this layer.[26, 29] The cyclic voltammograms for $K_3[Fe(CN)_6]^{3+/4+}$ on bare Au, Lip-NHS/Au, and Ethanolamine blocked TLR4/MD-2/Lip-NHS/Au electrodes in 5 mM $K_3[Fe(CN)_6]^{3+/4+}$ in 100 μM borate buffer (pH 7.4) have been shown in Fig. 2A. A reversible redox peak with the redox peak currents of -54 and 54 μA was observed for the bare gold electrode. The redox peak was decreased as a result of the formation of a Lip-NHS layer on the Au surface to -39 and 39 μA, respectively. The immobilization of TLR4/MD-2 complexes on the Lip-NHS/Au electrode lead to further decrease in the redox peak currents to -25 and 25 μA. ΔEp; the separation between two peak potentials was measured to be

0.068 V (bare gold), 0.141 V (Lip-NHS/Au), and 0.528 V (Ethanolamine/TLR4/MD-2/Lip-NHS/Au). The broadening of ΔEp and the decrease in the redox peak currents after each step of surface modification can be attributed to the blocking effect of each monolayer which inhibits the diffusion of $[Fe(CN)_6]^{3-/4-}$ anions. This result indicates successful modification of the Lip-NHS/gold electrode surface by TLR4/MD-2. Fig. 2B and C illustrates the cyclic voltammograms of bare Au and Ethanolamine/TLR4/MD-2/Lip-NHS/Au as a function of the scan rate in the range of 30 to 120 mV/s, respectively. The peak currents were dependent on the scan rate (with a linear relationship with the square root of the scan rate). This is an indication that the electrochemical reaction is diffusion-controlled which according to Yeo et al.[30] and Kaushik et al.[31] can be detailed as below:

I_a (bare gold electrode) = $6.75\ \nu^{1/2} - 6.81$, $R^2 = 0.993$ (3)

I_c (bare gold electrode) = $-5.93\ \nu^{1/2} + 2.13$, $R^2 = 0.996$ (4)

I_a (Ethanolamine/rhTLR4/MD-2/Lip-NHS/Au) = $2.17\nu^{1/2} + 5.60$, $R^2 = 0.998$ (5)

I_c (Ethanolamine/rhTLR4/MD-2/Lip-NHS/Au) = $-1.89\ \nu^{1/2} - 5.84$, $R^2 = 0.998$ (6)

Where ν (mV/s) is the scan rate, I_a (μA) is the oxidation peak current, and I_c (μA) is the reduction peak current. These results also show that the TLR4/MD-2 complex was successfully immobilized on the Lip-NHS/Au surface.

Investigation of the interaction of LPS with immobilized Lip-NHS

To investigate any possible interaction between the Lip-NHS linker molecules and LPS, Au surfaces modified with only Lip-NHS and blocked with 1 M ethanolamine in 50 mM Tris buffer pH 8.5 were incubated in different concentrations of LPS (*E. coli*). Fig. S1 shows that no significant change was observed in R_{ct} before and after incubation in LPS.

Interaction of immobilized TLR4/MD-2 with LPS

The interaction between TLR4/MD-2 immobilized on the Au surface with LPS from *E.coli* and *Salmonella* was studied individually and the binding of LPS to TLR4/MD-2 was investigated electrochemically in the presence of $[Fe(CN)_6]^{3-/4-}$ at pH 7.0. By increasing concentrations of LPS (both *E. coli* and *Salmonella*), an enhancement in the R_{ct} value was observed (Fig.3). EIS data were fitted to the appropriate equivalent circuit and the R_{ct} values were obtained (Fig. 3 and Tables S1 and S2). At LPS concentrations below 50 EU mL^{-1}, the R_{ct} was dependent on the LPS concentration and at 50 EU mL^{-1} LPS the surface was saturated. However the EIS data at 50 EU mL^{-1} and higher concentrations of LPS showed significantly less reproducibility and often a dramatic drop in the R_{ct} value. As the Lip-NHS linker showed no interaction with LPS (no

significant change in the electrochemical signal after the incubation of the Au electrodes modified only with Lip-NHS with different concentrations of LPS was observed) the decrease in impedance at high concentrations of LPS cannot be a result of linker aggregation and auto-oxidation.[32] The sudden drop in the impedance at high LPS concentrations however, can be attributed to the aggregation of the protein immobilized on the well-defined Au surface.[26, 33] Herein, the decrease in impedance was explained by the steric hindrance and conformational changes of the immobilized TLR4/MD-2 induced by the dimerization and extensive aggregation. Although the TLR4/MD-2 undergoes some level of aggregation when interacting with LPS as a part of its functional mechanism[22], , it is probably the extent of aggregation which at its maximum, will cause opening of pinpoints and exposure of the gold surface to the components of the redox probe. And the maximum aggregation happens when the TLR4/MD-2 immobilized on the Au surface is incubated at high concentrations of LPS. On the other hand, the enhancement in the R_{ct} as result of LPS binding can be attributed not only to the increase in the insulating layer thickness, which would partially inhibit the oxidation/reduction of the anionic marker ions ($[Fe(CN)_6]^{4-/3-}$), but also to the electrostatic repulsion between these anionic marker ions and the negatively charged LPS bound to the TLR4/MD-2 protein on the electrode surface.

Similar to Randle's circuit in the equivalent circuit used here, as the total current passing through the interface is the sum of the contributions from the faradaic process, i_f, and double-layer charging, i_c, these components are introduced in parallel.[34] Also as the double-layer capacitance

is almost a pure capacitance, it is represented in the equivalent circuit as the element C_{dl}. However, due to the complexity of the surface, which is modified by a protein complex consisting of two interacting proteins (TLR4/MD-2), and the nature of the analyte (LPS) which has both hydrophobic and hydrophilic parts, the equivalent circuit has been modified. Here, R_s is the solution resistance (the uncompensated resistance between the working and reference electrode) through which all the current must pass and so it is in series with the double layer capacitance and resistance, C_{dl} and R_{dl} (elements in parallel to each other) and in series with the film capacitance Q, charge transfer resistance, R_{ct} and Warburg impedance (Z_w) respectively.

C_{dl} is the double layer capacitance, which is formed between the electrode surface and the surrounding electrolyte. R_{dl} is referred to as the double layer resistance and is the resistance in the interfacial ionic charge transfer from the solution phase through the electrical double layer to electrode surface.[35] R_{ct} is the charge transfer resistance resulting from the transfer of the electron from the solution-based redox probe $[Fe(CN)_6]^{3-/4-}$ to the gold electrode surface through the TLR4/MD-2 and LPS monolayers. The film capacitance (Q) accounts for the capacitance of the gold surface modified with TLR4/MD-2 and after LPS binding.[36] The enhancement in the R_{ct} by the binding of LPS to the TLR4/MD-2 immobilized on gold surface as a result of increase in the thickness of the insulating layer and also repletion of the negatively charged components of the redox probe by the negatively charged analyte (LPS) bound to the surface is used to obtain the calibration curves.

Table 1 compares the analytical figures of merit for quantification of LPS from *E. coli* and *Salmonella* using calibration curves obtained from the R_{ct} data. The calibration curves obtained showed similar dynamic linear ranges and linearities for *E. coli* and *Salmonella* LPS samples.

The limit of detections calculated were 1.3×10^{-4} and 1.5×10^{-4} EU mL^{-1} for LPS from *E. coli* and *Salmonella*, respectively.

X-ray Photoelectron Spectroscopy (XPS) studies

Fig. 4. Illustrates the results for XPS studies. The C (1s) spectra of Lip-NHS (Fig. 4A) can be fitted by assumption of three atomic species with binding energies of 288.5 eV (carboxyl), 286.3 eV (carbonyl), and 284.8 eV (aliphatic carbon) on the surface. When TLR4/MD-2 covalently bonds to the Lip-NHS immobilized on Au, similar three atomic species can be resolved in the C (1s) spectra, such as 288.5 eV (carboxyl and amide), 286.1 eV (aromatic), and 284.7 (aliphatic). After the incubation of the electrodes pre-treated with TLR4/MD-2 through Lip-NHS linkers in LPS a single C (1s) species of binding energy of 285.3 eV (corresponding to aliphatic, aromatic and C-O carbon) predominates. After incubation of the electrodes in LPS the intensity of the peak centered at 288.6 eV corresponding to carboxyl and amide groups, remains mostly the same as in Lip-NHS and TLR4/MD-2. The significant area increase of LPS C1s suggests the increase of the coverage thickness (Fig. 4A). The N (1s) spectra (Fig. 4B) appear as a broad peak centered at 400.0 eV. Decrease in intensity of N(1s) peak after incubation in LPS in comparison with after immobilization of TLR4/MD-2 can be explained by the attenuation of the signal[37] from deeper (Lip-NHS and TLR4/MD-2) layers by the overlayer of LPS that contains

significantly less nitrogen. The S(2p) peaks (Fig. 4C) at 163.5 eV may be fit to the typical $2p_{1/2,3/2}$ spin–orbital splitting pattern. No oxidized sulfur species (reported at binding energy of 166–169 eV)[38] were detected. Similarly to N(1s) spectrum, the intensity of S(2p) peaks of LPS-covered TLR4/MD-2-modified electrodes is less than the corresponding intensity of TLR4/MD-2-modified electrode before incubation in LPS. Indeed, after LPS binding, thiol groups of Lip-NHS bound to the gold become too far away from the surface and thus their XPS response is attenuated. The thicknesses of overlayers were determined as previously reported.[39-40] Au 4d signals attenuation (I_s/I_0) has been used in this study to estimate the overlayer film thickness using the following relationship:[41-42]

$$t = (-\lambda\cos\theta)\ln(I_s/I_0) \quad (7)$$

where t is the thickness of the overlayer, λ is the effective attenuation length determined using the NIST Standard Reference Database[43] for Au $4d_{5/2}$ and Au $4d_{3/2}$ electrons, θ is the takeoff angle (here 5°), I_s is the substrate Au 4d signal intensity after modification, and I_0 is the substrate Au 4d signal intensity before modification. The thicknesses of the Lip-NHS/TLR4/MD-2 and Lip-NHS/TLR4/MD-2/LPS layers were found to be 2.2 nm and 3.7 nm, respectively (Scheme 2, Fig S2). These values are slightly smaller than the values determined by contact-mode AFM for

related layers[44] probably due to the stronger TLR4-LPS long-distance interactions resulting to better packing.

Quartz-Crystal Microbalance (QCM) measurements

The Quartz Crystal Microbalance (QCM) is a piezoelectric effect-based technique which is generally employed to characterize the adsorbed mass at a solid surface. As a result of application of an altering potential to the electrode, in the piezoelectric material, a shear stress is formed which causes the crystal to oscillate at a certain resonance frequency. A shift in the resonance frequency (Δf) is caused by the changes in the mass (Δm) bound to the surface of the crystal. If no significant damping effects by the environment are present, the Sauerbrey relation can be employed as below:

$$\Delta f = \frac{-2{f_0}^2 \Delta m}{A\sqrt{\mu\rho}} \quad (8)$$

where f_0 is the resonant frequency of crystal's fundamental mode, A is the area of the gold disk coated onto the crystal and ρ is the crystal's density (= 2.684 g/cm^3) and μ is the shear modulus of quartz (= 2.947 x 10^{11} g/cm*s^2). For the eq. (8) to be applicable the following conditions should

be fulfilled: (i) the mass adsorbed should be evenly distributed on the sensor surface. (ii) The mass adsorbed on the surface should be much smaller than the crystal mass and (iii) there should be perfect coupling between the adsorbed film on the sensor and the shear oscillation of the sensor.[45] 7.995 MHz QCM plates oscillating at the fundamental frequency were used to perform these measurements. The polished QCM plate was placed in the cell and the cell was filled with 500 μL 100 μM borate buffer pH 7.4 and the time course frequency changes were measured until a stable baseline was achieved. Then the change of the time course frequency on the addition of Lip-NHS, TLR4/MD-2 and LPS was monitored to investigate the immobilization and binding processes. Upon the addition of Lip-NHS on the surface to the bare electrode, the frequency decreased by ca. 80 Hz. After the addition of TLR4/MD-2, the frequency further decrease by ca 30 Hz. Binding of LPS to the TLR4/MD-2 immobilized on the gold surface lead to another decrease in frequency by 16 Hz (Fig. 5). Using the experimental parameters and these frequency changes to the change in mass (Δm) can be calculated as the adsorption of 179 ng, 70 ng and 32 ng of Lip-NHS, TLR4/MD-2 and LPS, respectively on the sensor surface.

Conclusion

The research reported here, describes the characterization of the Au surface modified with TLR4/MD-2 and investigates the interaction between immobilized TLR4/MD-2 and LPS with

the ultimate goal of using this interaction for LPS detection. Using TLR4/MD-2 as a component of the innate immune system as a bio-recognition element, provides a low-cost, fast and simple method for LPS detection with the possibility of miniaturization. The Au surfaces were successfully modified by TLR4/MD-2 through Lip-NHS linkers.

Using XPS and QCM the successful modification of the Au surfaces by TLR4/MD-2 and its interaction with LPS was confirmed. Investigation of the interaction between TLR4/MD-2 immobilized on Au surfaces and LPS show the applicability of using TLR4/MD-2-modified electrodes for LPS detection. These sensors demonstrate similar electrochemical behaviour for LPS from *E. coli* and *Salmonella* and therefore could not discriminate between two LPS samples from two different Gram-negative bacteria. One of the disadvantages of biosensor technologies for pathogen detection in general is their restrictively high specificity towards the analyte as a result of employing highly specific bio-recognition elements such as antibodies. These biosensors will fail to detect the analyte if it undergoes any change in its structure for instance mutation. The fact that TLR4/MD-2 interacts and binds to LPS as a molecular pattern of Gram-negative bacteria and not the Gram-negative bacteria themselves, TLR4/MD-2-modified electrodes can provide a global platform for detection of all Gram-negative bacterial contaminations.

Our current work is focused on using TLR4/MD-2 modified surfaces for the analysis of Gram-negative bacterial LPS in environmental aqueous samples such as lake or river waters. These studies will include testing of matrix effects and interferences and will be published in due time.

Acknowledgement

K. A. is the recipient of Ontario Graduate Scholarship (2015-2016). We thank NSERC for providing funding in the form of a Discovery Grant. We also thank the University of Toronto Scarborough for funding.

References

1. K. Amini and H.-B. Kraatz, *Reviews in Environmental Science and Bio/Technology*, 2014, **14**, 23-48.

2. A. Rydosz, E. Brzozowska, S. Górska, K. Wincza, A. Gamian and S. Gruszczynski, *Biosensors and Bioelectronics*, 2016, **75**, 328-336.

3. R. M. Hawk and A. M. Armani, *Biosensors and Bioelectronics*, 2015, **65**, 198-203.

4. J. Yang, P. Gao, Y. Liu, R. Li, H. Ma, B. Du and Q. Wei, *Biosensors and Bioelectronics*, 2015, **64**, 13-18.

5. Z. Lv, J. Liu, W. Bai, S. Yang and A. Chen, *Biosensors and Bioelectronics*, 2015, **64**, 530-534.

6. R. Chauhan, P. R. Solanki, J. Singh, I. Mukherjee, T. Basu and B. D. Malhotra, *Food Control*, 2015, **52**, 60-70.

7. S. G. Patching, *Biochimica et Biophysica Acta (BBA) - Biomembranes*, 2014, **1838**, 43-55.

8. C. E. Nwankire, A. Venkatanarayanan, T. Glennon, T. E. Keyes, R. J. Forster and J. Ducrée, *Biosensors and Bioelectronics*, 2015, **68**, 382-389.

9. C.-C. Wu, W.-C. Huang and C.-C. Hu, *Sensors and Actuators B: Chemical*, 2015, **209**, 61-68.

10. M. Barreiros dos Santos, S. Azevedo, J. P. Agusil, B. Prieto-Simón, C. Sporer, E. Torrents, A. Juárez, V. Teixeira and J. Samitier, *Bioelectrochemistry*, 2015, **101**, 146-152.

11. M. S. McClellan, L. L. Domier and R. C. Bailey, *Biosensors and Bioelectronics*, 2012, **31**, 388-392.

12. M. Cretich, A. Reddington, M. Monroe, M. Bagnati, F. Damin, L. Sola, M. S. Unlu and M. Chiari, *Biosensors and Bioelectronics*, 2011, **26**, 3938-3943.

13. S. El Ichi, F. Leon, L. Vossier, H. Marchandin, A. Errachid, J. Coste, N. Jaffrezic-Renault and C. Fournier-Wirth, *Biosensors and Bioelectronics*, 2014, **54**, 378-384.

14. M. Mujika, A. Zuzuarregui, S. Sánchez-Gómez, G. M. de Tejada, S. Arana and E. Pérez-Lorenzo, *J. Biotechnol.*, 2014, **186**, 162-168.

15. A. Hreniak, K. Maruszewski, J. Rybka, A. Gamian and J. Czyżewski, *Optical Materials*, 2004, **26**, 141-144.

16. D. Kato, S. Iijima, R. Kurita, Y. Sato, J. Jia, S. Yabuki, F. Mizutani and O. Niwa, *Biosensors and Bioelectronics*, 2007, **22**, 1527-1531.

17. K. Y. Inoue, K. Ino, H. Shiku and T. Matsue, *Electrochem. Commun.*, 2010, **12**, 1066-1069.

18. S.-J. Ding, B.-W. Chang, C.-C. Wu, C.-J. Chen and H.-C. Chang, *Electrochem. Commun.*, 2007, **9**, 1206-1211.

19. N. J. Gay and M. Gangloff, *Annu. Rev. Biochem.*, 2007, **76**, 141-165.

20. A. Poltorak, X. He, I. Smirnova, M.-Y. Liu, C. V. Huffel, X. Du, D. Birdwell, E. Alejos, M. Silva, C. Galanos, M. Freudenberg, P. Ricciardi-Castagnoli, B. Layton and B. Beutler, *Science*, 1998, **282**, 2085-2088.

21. R. Medzhitov, P. Preston-Hurlburt and C. A. Janeway, Jr., *Nature*, 1997, **388**, 394-397.

22. H. M. Kim, B. S. Park, J.-I. Kim, S. E. Kim, J. Lee, S. C. Oh, P. Enkhbayar, N. Matsushima, H. Lee, O. J. Yoo and J.-O. Lee, *Cell*, 2007, **130**, 906-917.

23. S. Viriyakosol, P. S. Tobias, R. L. Kitchens and T. N. Kirkland, *J. Biol. Chem.*, 2001, **276**, 38044-38051.

24. C. R. H. Raetz and C. Whitfield, *Annu. Rev. Biochem.*, 2002, **71**, 635-700.

25. W. Liu, M. Howarth, A. B. Greytak, Y. Zheng, D. G. Nocera, A. Y. Ting and M. G. Bawendi, *Journal of the American Chemical Society*, 2008, **130**, 1274-1284.

26. K. Amini, N. W. C. Chan and H.-B. Kraatz, *Analytical Methods*, 2014, **6**, 3322-3328.

27. M.-H. Sorouraddin, K. Amini, A. Naseri and M.-R. Rashidi, *cent.eur.j.chem.*, 2010, **8**, 207-213.

28. J. C. Miller and J. N. Miller, eds., *Statistics for Analytical Chemistry*, 2nd edn., Wiely, New York, 1988.

29. S. Prabhulkar, S. Alwarappan, G. Liu and C.-Z. Li, *Biosensors and Bioelectronics*, 2009, **24**, 3524-3530.

30. T. Y. Yeo, J. S. Choi, B. K. Lee, B. S. Kim, H. I. Yoon, H. Y. Lee and Y. W. Cho, *Biosensors and Bioelectronics*, 2011, **28**, 139-145.

31. K. Ajeet, S. Pratima Rathee, A. Anees Ahmad, A. Sharif and M. Bansi Dhar, *Nanotechnology*, 2009, **20**, 055105.

32. N. Li, A. Brahmendra, A. J. Veloso, A. Prashar, X. R. Cheng, V. W. S. Hung, C. Guyard, M. Terebiznik and K. Kerman, *Anal. Chem.*, 2012, **84**, 3485-3488.

33. A. Sethuraman and G. Belfort, *Biophys. J.*, 2005, **88**, 1322-1333.

34. A. J. Bard, L.R. Faulkner, Electrochemical Methods; fundementals and applications, 2nd Edition, John Wiley & Sons Inc. 2001.

35. P. Długołęcki, Ogonowski, S.J. Metzb, M. Saakesb, K. Nijmeijer, M. Wesslinga, *J. Membr. Sci.*, 2010, **349**, 369-379.

36. Z. She, K. Topping, M. H. Shamsi, N. Wang, N. W. C. Chan, H.-B. Kraatz, *Anal. Chem.*, 2015, **87(8)**, 4218-4224.

37. J. Tong and T. J. McIntosh, *Biophys. J.*, **86**, 3759-3771.

38. J. Poppenberg, S. Richter, E. Darlatt, C. H. H. Traulsen, H. Min, W. E. S. Unger and C. A. Schalley, *Surf. Sci.*, 2012, **606**, 367-377.

39. A. A. Azmi, I. I. Ebralidze, S. E. Dickson and J. H. Horton, *J. Colloid Interface Sci.* , 2013, **393**, 352-360.

40. A. Gulino, F. Lupo, M. E. Fragalà and S. L. Schiavo, *J. Phys. Chem. C*, 2009, **113**, 13558-13564.

41. I. I. Ebralidze, M. Hanif, R. Arjumand, A. A. Azmi, D. Dixon, N. M. Cann, C. M. Crudden and J. H. Horton, *J. Phys. Chem. C*, 2012, **116**, 4217-4223.

42. C. J. Powell and A. Jablonski, *J. Electron. Spectrosc. Relat. Phenom.*, 2001, **114–116**, 1139-1143.

43. C. J. Powell and A. Jablonski, National Institute of Standards and Technology, Gaithersburg, Maryland, USA, 2011, vol. Version 1.3.

44. J. Tong and T. J. McIntosh, *Biophys. J.*, 2004, **86**, 3759-3771.

45. L. Wang, I. Siretanu, M. H. G. Duits, M. A. C. Stuart and F. Mugele, *Colloids and Surfaces A: Physicochemical and Engineering Aspects*, 2016, **494**, 30-38.

Schemes

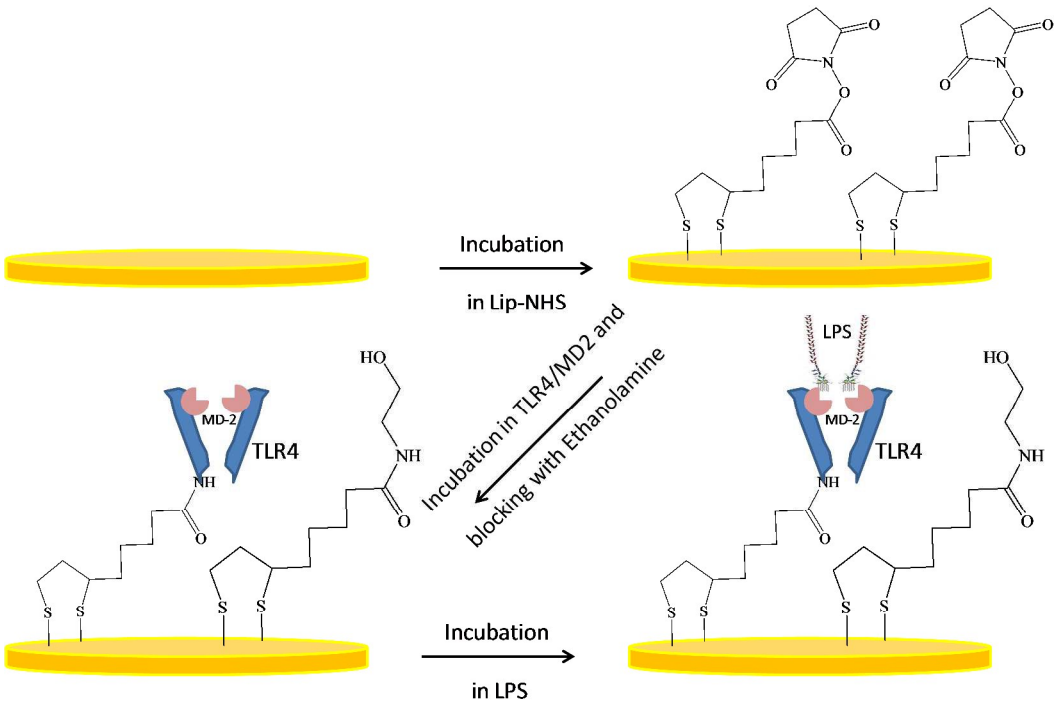

Scheme 1 Schematic illustration of the construction of a TLR4/MD-2-modified Au sensor and the electrochemical assay using this sensor for detection of LPS.

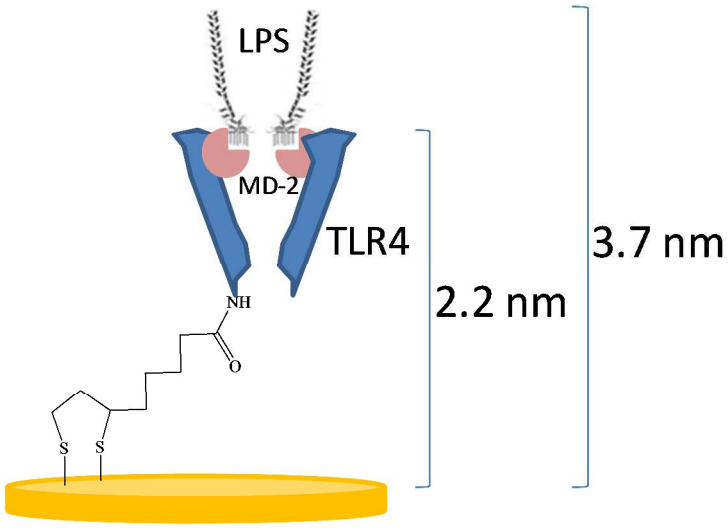

Scheme 2 Schematic illustration of the thicknesses of the Lip-NHS/TLR4/MD-2 and Lip-NHS/TLR4/MD-2/LPS layers on the Au surface obtained using XPS as described previously [39-40].

Figures

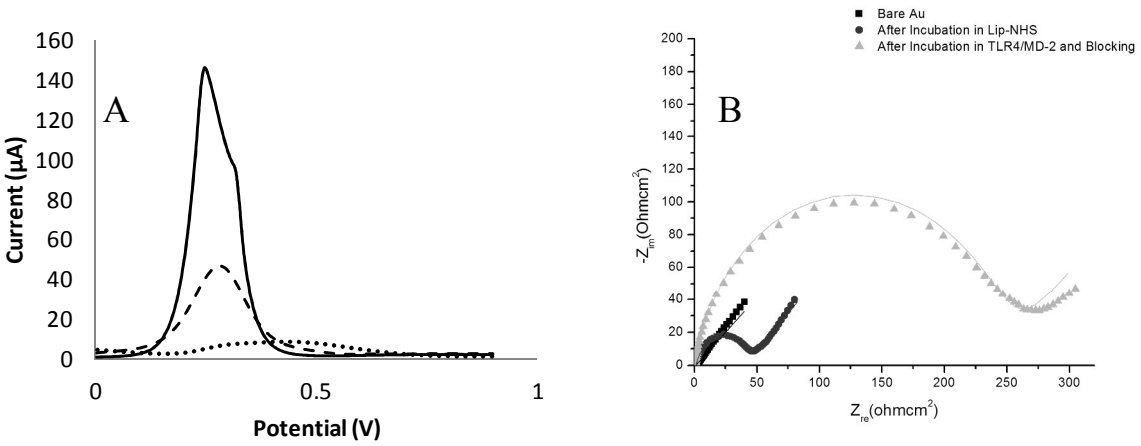

Fig. 1 (A) square wave voltammetry (SWV) for bare Au (—), after incubation in Lip-NHS (----), after incubation in TLR4/MD-2 and blocking with ethanolamine (.....) and (B) electrochemical impedance spectroscopy for bare Au (●), Au electrode after modification with Lip-NHS (■), and TLR4/MD-2 and blocking with ethanolamine (▲). Data points show the experimental results while the solid lines show the calculated results.

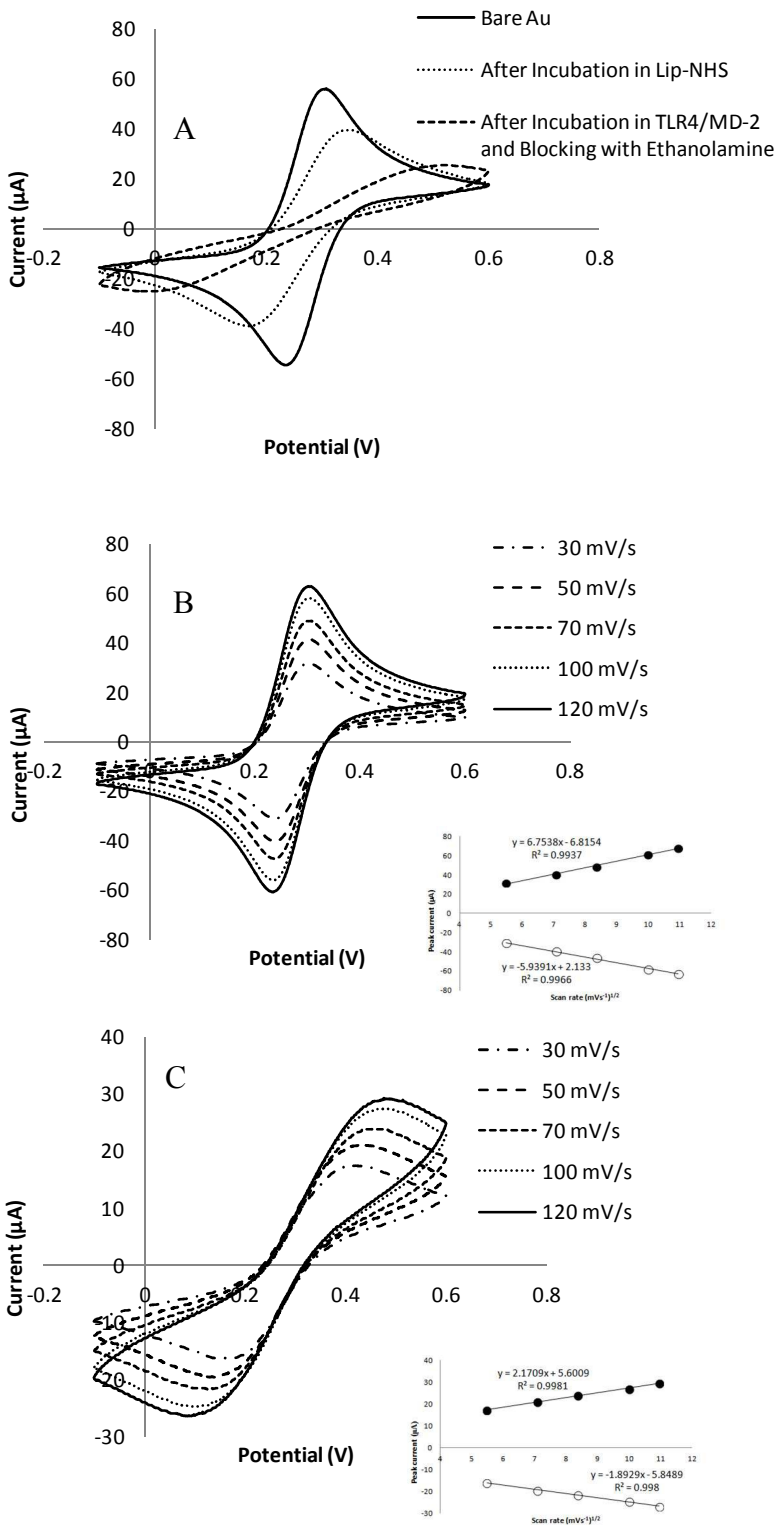

Fig. 2 Cyclic voltammograms obtained in 5 mM $[Fe(CN)6]^{3-/4-}$ and 100 nM borate buffer. (A) Bare Au, Au/Lip-NHS, and Au/Lip-NHS/TLR4/MD-2/Ethanolamine electrodes at a scan rate of 100 mV/s, (B) Bare Au and (C) Au/Lip-NHS/TLR4/MD-2/Ethanolamine sensors at different scan rates. The insets show the plots of the peak current (µA) vs. the square root of scan rate (mV/s).

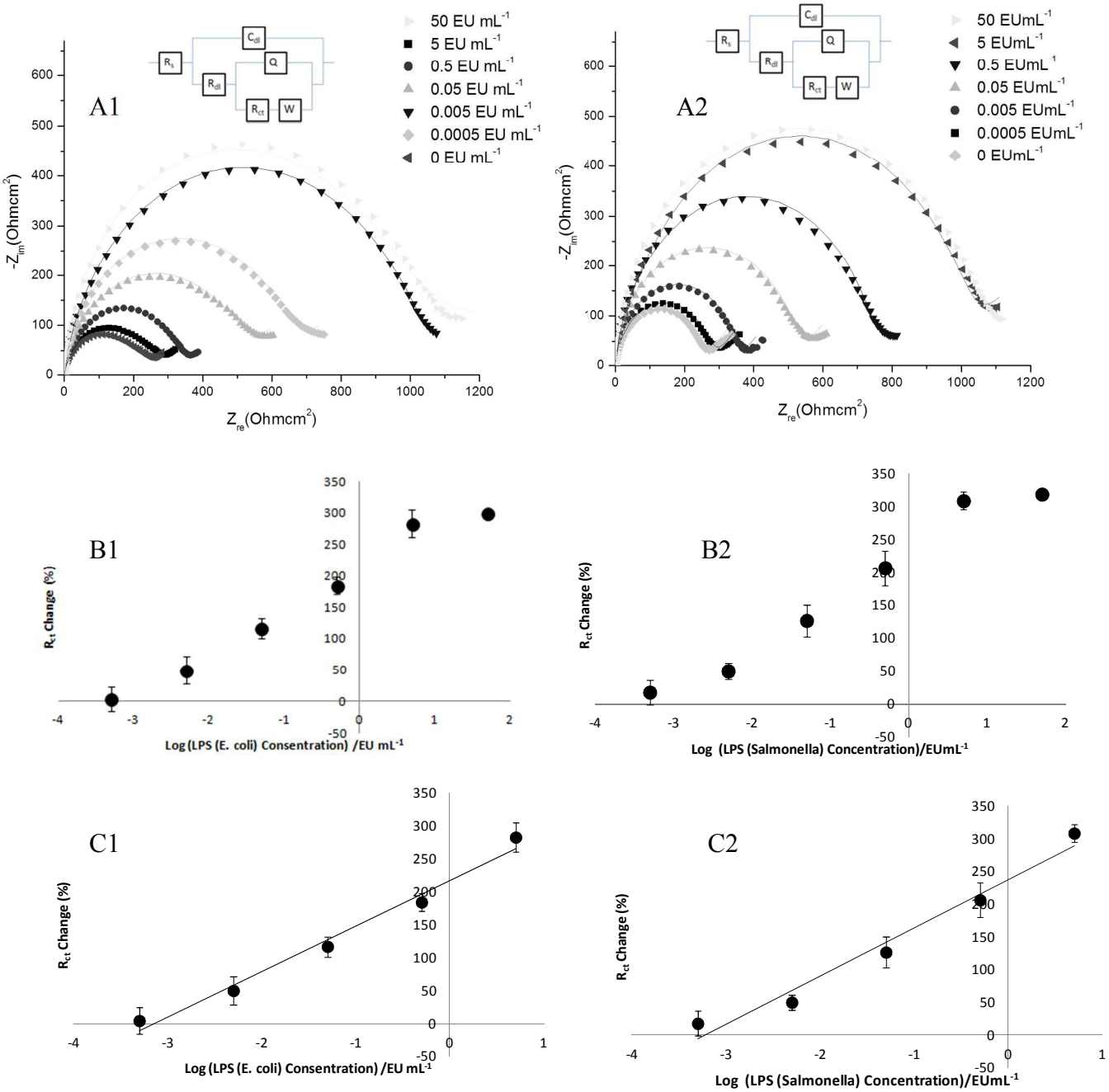

Fig. 3 (A1) and (A2) show the EIS obtained for the incubation of TLR4/MD-2-modified Au sensors in different concentrations of LPS from *E.coli* and *Salmonella* respectively in the presence of 5 mM $[Fe(CN)_6]^{3-/4-}$ in 100mM borate buffer, pH 7.4. Data points show experimental results while solid lines represent the spectra calculated for the equivalent circuit shown as inserts. (B1) and (B2) illustrate the R_{ct} values obtained by fitting the EIS data obtained after incubation of the TLR4/MD-2-modified Au sensors in different concentrations of LPS from *E.coli* and *Salmonella* respectively. (C1) and (C2) depict the calibration curves obtained from the R_{ct} data for LPS from *E.coli* and *Salmonella* respectively.

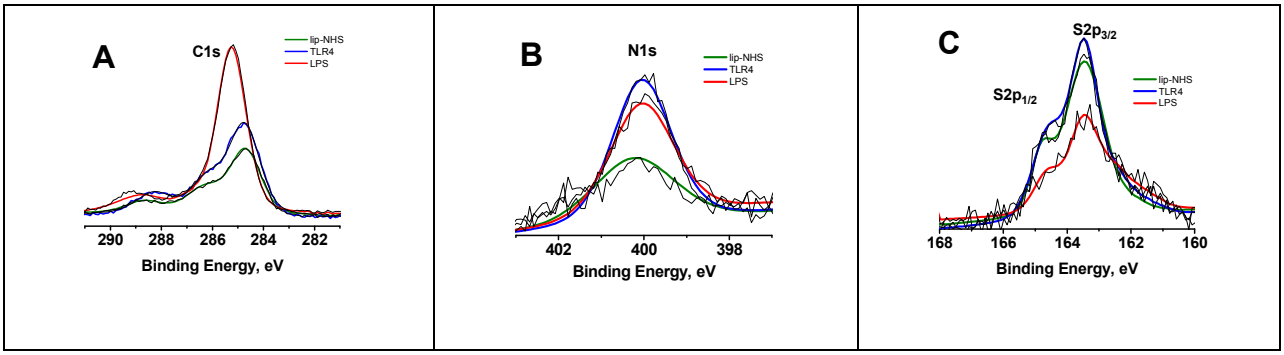

Fig. 4 Representative XPS data for modified gold surfaces (A) C(1s), (B) N(1s), and (C) S(2p). The black line shows the experimental data, while the colored lines are the overall fitted spectra. See the main text for specific peak assignments.

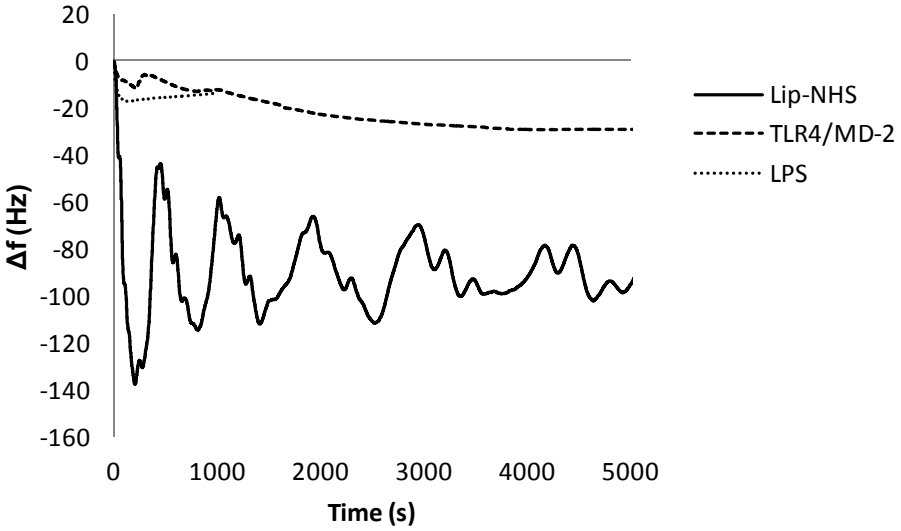

Fig. 5 Frequency changes in response to the addition of the Lip-NHS linker solution, TLR4/MD-2 protein solution and LPS (E. coli) solution. Samples were added into 500 μL of a buffered solution (100 mM borate buffer (pH 7.4)) in the QCM cell at room temperature (final concentrations of the Lip-NHS, TLR4/MD-2 and LPS were 1 mM, 1 μM and 5 EU mL^{-1}).

Tables

Table 1. Analytical figures of merit for quantification of LPS from E. coli and Salmonella using calibration curves obtained from the R_{ct} data.

Parameters	**LPS from *E. coli***	**LPS from *Salmonella***
Dynamic linear range ($EUmL^{-1}$)	$5\times10^{-4} - 5$	$5\times10^{-4} - 5$
Correlation coefficient (R^2)	0.9824	0.9722
Limit of detection ($EUmL^{-1}$), n=5	1.3×10^{-4}	1.5×10^{-4}
Equation of calibration curve (R_{ct} versus $EUmL^{-1}$ of analyte)	y = 69.179x + 217.49	y = 73.856x + 237.98